Int J Adv Manuf Technol (2013) 67:957–967
DOI 10.1007/s00170-012-4540-2

ORIGINAL ARTICLE

Prediction of surface roughness and cutting zone temperature in dry turning processes of AISI304 stainless steel using ANFIS with PSO learning

Mehmet Aydın · Cihan Karakuzu · Mehmet Uçar · Abdulkadir Cengiz · Mehmet Ali Çavuşlu

Received: 1 June 2012 / Accepted: 2 October 2012 / Published online: 16 October 2012

Abstract This paper presents an approach for modeling and prediction of both surface roughness and cutting zone temperature in turning of AISI304 austenitic stainless steel using multi-layer coated (TiCN+TiC+TiCN+TiN) tungsten carbide tools. The proposed approach is based on an adaptive neuro-fuzzy inference system (ANFIS) with particle swarm optimization (PSO) learning. AISI304 stainless steel bars are machined at different cutting speeds and feedrates without cutting fluid while depth of cut is kept constant. ANFIS for prediction of surface roughness and cutting zone temperature has been trained using cutting speed, feedrate, and cutting force data obtained during experiments. ANFIS architecture consisting of 12 fuzzy rules has three inputs and two outputs. Gaussian membership function is used during the training process of the ANFIS. The surface roughness and cutting zone temperature values predicted by the PSO-based ANFIS model are compared with the measured values derived from testing data set. Testing results indicate that the predicted surface roughness and cutting zone temperature are in good agreement with measured roughness and temperature.

Keywords ANFIS · PSO · Surface roughness · Cutting temperature

M. Aydın (✉)
The Program of Mechanics, Vocational School of Higher Education, Bilecik Şeyh Edebali University, Campus of Gülümbe, 11210 Bilecik, Turkey
e-mail: mehmet.aydin@bilecik.edu.tr

C. Karakuzu
Department of Computer Engineering, Faculty of Engineering, Bilecik Şeyh Edebali University, Campus of Gülümbe, 11210 Bilecik, Turkey

M. Uçar · A. Cengiz
Department of Mechanical Education, Faculty of Technical Education, Kocaeli University, Campus of Umuttepe, 41380 Kocaeli, Turkey

M. A. Çavuşlu
Department of Computer Engineering, Natural and Applied Sciences Institute, Kocaeli University, Campus of Umuttepe, 41380 Kocaeli, Turkey

1 Introduction

Metal cutting is one of the most widely used manufacturing technologies today. It is also an important research topic due to complex nature of process. Among metal cutting techniques, turning is typically used to shape of cylindrical parts. Cutting parameters such as cutting speed and feedrate play critical roles on cutting temperature and surface roughness in turning processes. Surface roughness, which is used for evaluating the product quality, is an important performance characteristic in turning processes. In metal cutting, temperature strongly affects mechanical properties of workpiece material and forces on tool and workpiece, and it causes wear on tool rake and flank faces. Furthermore, a high temperature has a considerable influence on accuracy of metal cutting process.

Austenitic stainless steels are always considered as difficult materials to machine than carbon and low alloy steels because of their high toughness, low thermal conductivity, high ductility, and high work hardening rate. In other words, their machinability is low due to these main characteristics. Work hardening rate and low thermal conductivity are recognized as the most important characteristics in the poor machinability of austenitic stainless steel. On the other hand,

these characteristics cause the formation of built-up edge (BUE) and segmental chips in machining. The presence of BUE affects machinability behavior in the machining of austenitic stainless steels by causing decreased surface roughness and tool life. Austenitic stainless steels also have the most corrosion resistant when compared to other classes of stainless steel. However, for austenitic stainless steels, it is difficult to combine the improvement of corrosion resistance with good machinability. The machinability studies of austenitic stainless steels were carried out over a wide range of machining parameters in turning, milling, and drilling operations. Fernández-Abia et al. [1] investigated the effect of very high cutting speeds to analyze behavior of workpiece material and cutting tool in dry turning of AISI303 austenitic stainless steel. In the other research carried out by Fernández-Abia et al. [2], the authors proposed a mechanistic approach to determine the force coefficients in the turning of AISI303 stainless steels at high cutting speeds. Dolinšek [3] conducted a study to find the reasons of difficulties in machining stainless steel. Based on this study, the author pointed out all problems connected with the machinability of these steels and particularities in the chip transformation mechanism on the cutting edges. Korkut et al. [4] aimed to determine the optimum cutting speed by investigating tool wear and surface roughness in turning AISI304 stainless steel using carbide cutting tools. Ciftci [5] presented the effects of cutting tool coating, cutting speed, and workpiece materials on surface roughness and cutting forces in dry turning of AISI304 and AISI316 stainless steels using two different grades of coated carbide tools.

Fuzzy logic (FL) is a theory used to describe the relationship between system inputs and outputs. It is widely used to develop rule-based expert systems in modeling of complex processes that cannot be modeled analytically under various assumptions. Hashmi et al. [6] described an adjustment approach based on a FL model to select cutting speeds in turning of various wrought carbon steels. Nandi [7] designed a Takagi–Sugeno–Kang-type fuzzy logic controller to model input–output relationship in ultraprecision turning of annealed aluminum alloy (LY 12). Kirby et al. [8] developed a fuzzy-nets-based in-process adaptive surface roughness control system for turning operations of 6061-T6511 aluminum alloy rods using tool vibrations. Non-conventional approaches were also developed to model and simulate machining processes. The fuzzy adaptive network (FAN) is an ideal non-conventional approach to model a machining process. Jiao et al. [9] used the FAN to model surface roughness in turning of 1,045 cold rolled steel. Other approaches used for modeling metal cutting processes can be summarized as follows: Ho et al. [10] proposed a method using an ANFIS to accurately establish the relationship between the features of surface image and the actual surface roughness in turning of S45C steel bars. Abburi and Dixit [11] developed a knowledge-based system with the help of neural network and fuzzy set theory for prediction of surface roughness in turning of rolled steel bars containing about 0.35 % carbon. Evolutionary fuzzy systems have also been considered to solve the different problems. Kumar et al. [12] applied a hybrid neural network model called as recurrent self-organizing neuro fuzzy network model (SONFN) to predict the flow stress for carbon steels. The main constituents of recurrent SONFN are neuro fuzzy network (NFN) and polynomial neural network (PNN). Based on SONFN, Anand et al. [13] also proposed a new methodology to solve complex manufacturing system design problems, incorporating of two soft computing tools: NFN and PNN. Rai et al. [14] used a fuzzy-genetic algorithm (GA)-based approach to model the complex machine-tool selection and operation problems.

In the past several years, PSO technique has been successfully applied to solve machining problems. Tandon et al. [15] proposed a technique based on PSO to optimize cutting conditions in end milling. This technique was suitable for predicting cutting forces using artificial neural network model. Lee et al. [16] established a PSO methodology to obtain optimum machining parameters for silicon carbide grinding. The authors concluded that PSO methodology was relatively better in comparison with GA. Srinivas et al. [17] proposed a methodology for selecting optimum machining parameters in multi-pass turning subjected to several constraints. For this purpose, PSO was used to obtain optimal set of cutting parameters. Yıldız [18] developed a new optimization approach for multi-pass turning operations and design optimization problems by hybridizing PSO algorithm and receptor editing property of immune system. Raja and Baskar [19] developed a mathematical model for surface roughness prediction using PSO on the basis of experimental results. PSO was used to optimize machining parameters and get desired surface roughness in face milling of aluminum material.

As can be seen from the literature review above, there have not been any studies on prediction of both surface roughness and cutting zone temperature. Moreover, due to the above-mentioned machining problems of austenitic stainless steels, it is essential to have the knowledge about surface roughness and cutting temperature, arising in the turning of austenitic stainless steels, prior to machining operations to attain higher productivity levels. Thus, one of austenitic stainless steels used in manufacturing machinery parts, food, and chemical industry equipments requiring high corrosion resistance, AISI304, is selected as test material in this study. This

paper proposes a novel PSO-based ANFIS model effectively to predict both surface roughness and the cutting zone temperature in turning processes. ANFIS proposed by Jang [20] is a powerful tool and have been successfully used in many studies for modeling or prediction relationship between input–output data. Therefore, in this research, an ANFIS model is presented to predict surface roughness and cutting zone temperature in dry turning of AISI304 austenitic stainless steel using multilayer coated tungsten carbide tools. The proposed model is trained using PSO learning algorithm and then its performance is tested for verification data set.

2 Experimental procedures

2.1 Workpiece material, cutting tool, and equipment

All the turning experiments have been carried out in dry cutting conditions on a TEZSAN SN50CX2000 industrial type of lathe machine having a maximum spindle speed of 6,000 rpm and a maximum feedrate of 6.40 mm/rev. Figure 1 shows the set-up of turning operation.

The experiments have been performed by single point turning of AISI304 austenitic stainless steel cylindrical-shaped bars with a diameter of 80 mm and a length of 250 mm. The used cutting tool is tungsten carbide coated with TiCN+TiC+TiCN+TiN. The carbide tools are commercially available inserts of ISO designation of CNMG120408. These inserts with chip breaker were rigidly clamped onto a PCLNR/L 2525 M12 type tool holder resulting in negative rake angle (γ=−5°) and side cutting edge angle (K_r) of 90°.

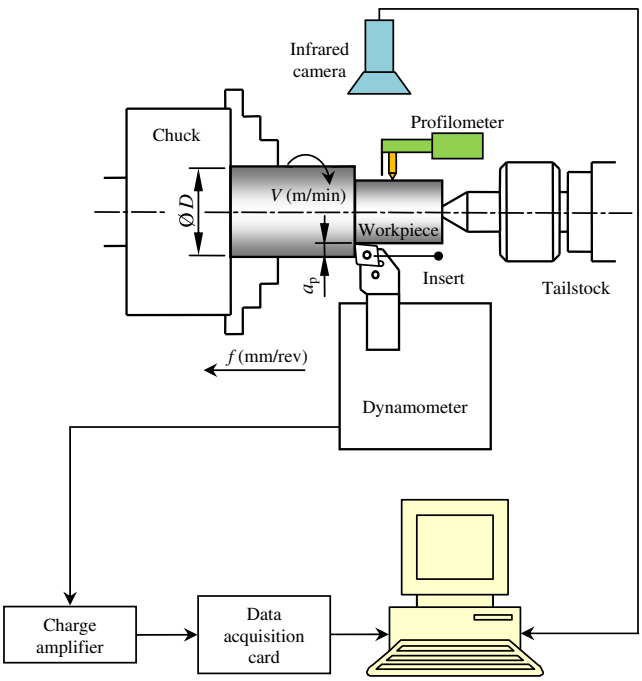

Fig. 1 Schematic representation of the experimental set-up used in this work

2.2 Measurement of cutting force

Cutting forces generated on tool during the turning have been collected using a piezoelectric force dynamometer (Kistler type 9257A), which is connected to a charge amplifier and data acquisition device. The measured forces are average tangential force components (F_c) in the direction parallel to relative velocity of tool and workpiece. Calibration of the device is made before the cutting experiments by applying known weights onto the insert. The signal acquisition has been realized with a Window-based LabVIEW software installed on the computer. The average force obtained from the force values collected during experiments is used for the purpose of ANFIS system training and testing.

2.3 Measurement of cutting zone temperature

Cutting temperature is one of the most important parameters in determining the cutting performance and tool life. However, measurement of temperature in metal cutting are too difficult due to a narrow shear band, chip obstacles, and the nature of the contact phenomena between tool and chip. Therefore, the practical methods have been developed for measurement of temperature in the machining operations. The infrared (IR) camera technique is one of ways of measuring cutting temperature. It is commonly used to measure the cutting temperatures since the IR camera technique has many advantages including: fast response, no adverse effects on temperatures and materials and no physical contact with the heat source, making it a very useful instrumentation. In this technique, the surface temperature of the body is measured based on its emitted thermal energy. However, the exact surface emissivity is an important disadvantage in the temperature measurements with the IR camera technique.

In this work, an IR digital camera (Model FLIR ThermaCAM^{TM} E45) is used to measure the cutting temperature. The measured temperature is the maximum temperature in the cutting zone. The IR camera is placed above the rake face of the tool to measure the maximum temperature of the cutting zone. The set-up for the experiments is shown in Fig. 1. The temperature measurement results in degrees Celsius are images of heat radiation. Then, all the image data are analyzed by a FLIR SYSTEMS QuickReport 1.2 control software and thus the maximum cutting zone temperature is determined for each experiment. Figure 2 shows an IR image of a cutting process.

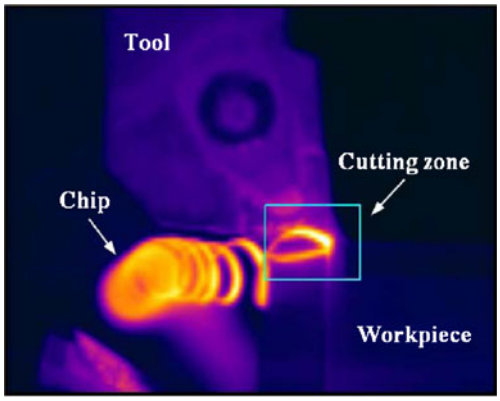

Fig. 2 An IR image obtained in the turning of AISI304 stainless steel

2.4 Measurement of surface roughness

On the machined surface, the roughness is measured by a Mahr Marsurf PS1 profilometer. The average roughness (R_a), commonly used in industries, in micron has been used. The measurements have been repeated at least three times in the axial direction and the average value has been used for investigation.

3 Experimental design

Experiments have been conducted to machine AISI304 stainless steel materials using multi-layer coated tungsten carbide tools in dry cutting conditions. During experiments critical parameters, the cutting speeds (V) and the feedrates (f), are varied to obtain a prediction model of surface roughness and maximum cutting zone temperature. As shown in Table 1, the cutting speed has four levels for training data set: 30, 55, 110, and 220 m/min. For purpose of testing, the cutting speed has four different levels, including 45, 75, 130, and 190 (meter per minute). The feedrate has three levels for purposes of training and testing: 0.05, 0.08, and 0.11 (millimeter per revolution). Because cutting tool is less affected than depth of cut and to make easy selection of cutting parameters, depth of cut (a_p) is set at 0.75 (millimeter) throughout the experiments. Based on the cutting parameter combinations, turning experiments have been carried out. In addition, the cutting force is one of the most important physical variables embodying process information in machining. This information can be used to assist in prediction of machining attributes such as surface roughness and cutting temperature. Therefore, the cutting forces obtained from the experiments are used to train ANFIS model using PSO algorithm and to verify the accuracy of the prediction model as the third parameter along with cutting speed and feedrate parameters.

Table 1 Cutting conditions

Cutting speed (V), m/min	30, 55, 110, 220 (for training data set)
	45, 75, 130,190 (for testing data set)
Feed rate (f), mm/rev	0.05, 0.08, 0.11
Depth of cut (a_p), mm	0.75
Cutting fluid	dry

4 The proposed ANFIS architecture

The architecture of ANFIS system is shown in Fig. 3. There are three inputs (V, f, and F_c) and two outputs (R_a and T_z). This system consists of five layers, namely, fuzzification layer, product layer, normalized layer, rule layer, and defuzzification or output layer as shown in Fig. 3.

Layer 1 is the fuzzification layer. Every node in this layer is an adaptive node with a membership function: $O_{1,i} = \mu_{A_i}(V)$, for i=1, …, m, $O_{1,j} = \mu_{B_j}(f)$, for j=1, …, m and $O_{1,k} = \mu_{C_k}(F_c)$, for k=1, …, m, where V, f, and F_c are the input of nodes A_i, B_j, and C_k, respectively. A_i, B_j, and C_k are the membership functions (MFs), and m is the number of MFs for each input parameter. In other words, $O_{1,i}$, $O_{1,j}$, and $O_{1,k}$, which are output functions of this layer, are the membership degrees ($\mu_{A_i}(V)$, $\mu_{B_j}(f)$, and $\mu_{C_k}(F_c)$) of the related inputs. Here, it is chosen Gaussian MFs given by Eq. (1).

$$\mu_{z_i}(Z) = \exp\left[-\left(\frac{Z - c_{z,i}}{\sigma_{z,i}}\right)^2\right],\ i = 1, \ldots, m \tag{1}$$

where the value of $Z \in \{V, f, F_c\}$ is the input, and $\{\sigma_{z,i}, c_{z,i}\}$ is the standard deviation (SD) and center parameters of the Gaussian MF, respectively. These parameters in this layer are referred to as premise or MF parameters.

Layer 2 is the product layer. Every node in this layer is a node labeled Π, which multiplies all of the incoming signals and sends it to its output. The outputs of this layer (w_1, w_2, …, w_{12}) are firing strength of the rules. For instance, $O_{2,n} = w_n = \mu_{A_i}(V) \cdot \mu_{B_j}(f)$, for n=1, 2, …, 12, where $O_{2,n}$ denotes the output of Layer 2.

Layer 3 is the normalized firing strength layer. Every node in this layer is a node labeled N. The nth node calculates the ratio of the nth rule's firing strength to the sum of all rules' firing strengths as given in Eq. (2):

$$O_{3,n} = \overline{w}_n = \frac{w_n}{w_1 + w_2 + \ldots + w_{12}},\ n = 1, 2, \ldots, 12 \tag{2}$$

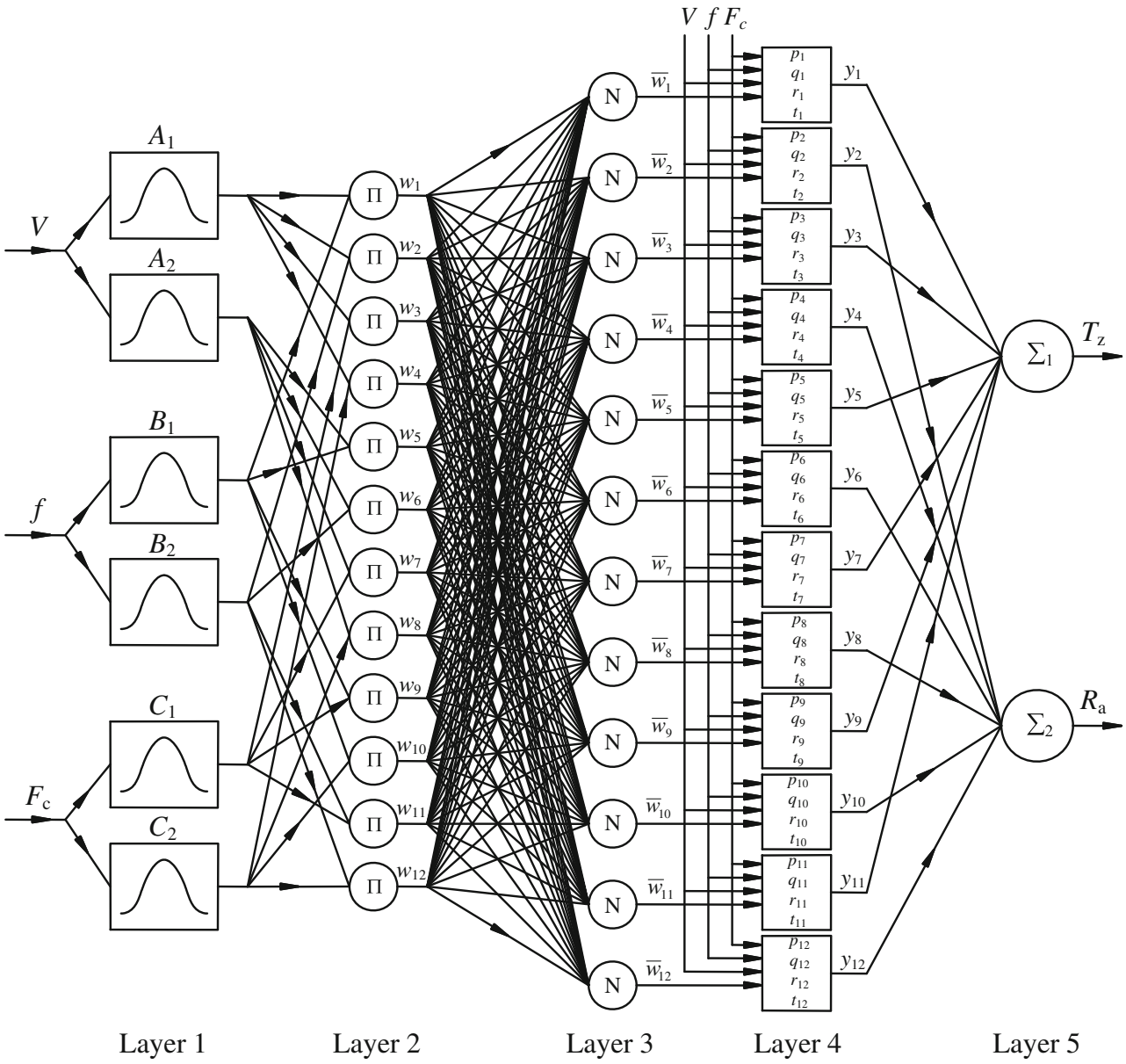

Fig. 3 Architecture of ANFIS system

where $O_{3,n}$ denotes the output of the nth node in Layer 3. Outputs of this layer are called *normalized firing strengths*. A typical rule can be expressed as: R_n: if V is A_i and f is B_j and F_c is C_k then $y_n = p_n V + q_n f + r_n F_c + t_n$.

Layer 4 is the rule layer. Every node in this layer is an adaptive node and the output of a node is calculated using $O_{4,n} = \overline{w}_n(p_n V + q_n f + r_n F_c + t_n)$, n=1, 2, …, 12, where $\overline{w}_n$ is the output of layer 3 and $\{p_n, q_n, r_n, t_n\}$ are rule parameters or so-called consequent or rule parameters of the nth rule. $O_{4,n}$ denotes the output of the nth node in layer 4.

Layer 5 is the defuzzification or output layer. The two nodes in this layer are nodes labeled $\sum$ that computes the outputs as the summation of incoming signals: Here, the first node is the first output for cutting zone temperature. The second node is also the second output for surface roughness.

5 Particle swarm optimization algorithm

Particle swarm optimization (PSO) is a population-based stochastic optimization technique first introduced by Eberhart and Kennedy [21]. The optimization procedure starts with randomly assigned a population of particles or solutions in the search space and then searches for optima by iteratively updating generations. Each particle is updated based on two important particles. The first

one, called "pbest", is the own best solution that has achieved so far by each particle. The other one, called "gbest", is the overall best one obtained so far among all the particles in the population. The basic flowchart of PSO algorithm is shown in Fig. 4.

5.1 PSO operations

In the PSO algorithm, the position of the *i*th particle is described by its vector position in the search space as given in Eq. (3):

$$\overrightarrow{p}_i = [p_{i1}\ p_{i2}\ p_{i3}\ \ldots\ p_{iN}] \tag{3}$$

where i is index of a particle in the swarm and N is the dimension of the search space. Each particle's position is evaluated as a possible candidate solution. The rate of change in the particle's position is called velocity and it is represented by Eq. (4) for the *i*th particle:

$$\overrightarrow{v}_i = [v_{i1}\ v_{i2}\ v_{i3}\ \ldots\ v_{iN}] \tag{4}$$

Each particle memorizes its own best position that it has discovered so far, called as the local best (pbest) particle which is represented by Eq. (5):

$$\overrightarrow{p}_b = [p_{b1}\ p_{b2}\ p_{b3}\ \ldots\ p_{bN}] \tag{5}$$

The population is called "swarm". The swarm also knows a record of the best position so far discovered among all the particles in the population, this is called as the global best (gbest) particle which is represented by Eq. (6):

$$\overrightarrow{g}_b = [g_{b1}\ g_{b2}\ g_{b3}\ \ldots\ g_{bN}] \tag{6}$$

After each particle and global best values are evaluated in each iteration of the PSO algorithm, particle velocity is computed to determine the position of particle for the next iteration. Particle velocity computing function Eq. (7) proposed by Çavuşlu et al. [22] have been adopted to compute the new velocity of each particle in this paper. Çavuşlu et al. [22] propose the additional parameter $\{\alpha_3\lambda(n)\}$ on the right-hand side of Eq. (7) as follows:

$$v_i(n+1) = \xi\left[v_i(n) + \alpha_1 r_1\left(p_{b,i} - p_i(n)\right) + \alpha_2 r_2\left(g_b - p_i(n)\right)\right] + \{\alpha_3\lambda(n)\} \tag{7}$$

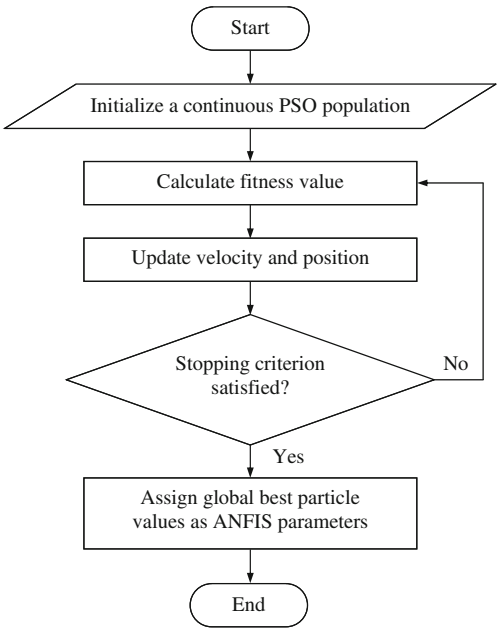

Fig. 4 Flowchart of the particle swarm optimization

Table 2 Experimental parameters and training data set

Experiment no.	Input parameters			Output parameters	
	V (m/min)	f (mm/rev)	F_c (N)	R_a (μm)	T_z (°C)
1	30	0.05	174	1.60	135.9
2	30	0.08	232	1.48	150.5
3	30	0.11	258	1.39	161.3
4	55	0.05	177	1.51	161.8
5	55	0.08	236	1.32	180.4
6	55	0.11	292	1.18	190.8
7	110	0.05	159	1.37	181.7
8	110	0.08	222	1.32	192.7
9	110	0.11	272	1.21	201.3
10	220	0.05	162	1.14	204.9
11	220	0.08	216	1.37	210.6
12	220	0.11	251	1.24	229.7

Table 3 Experimental parameters and testing data set

Experiment no.	Input parameters			Output parameters	
	V (m/min)	f (mm/rev)	F_c (N)	R_a (μm)	T_z (°C)
1	45	0.05	168	1.53	148.6
2	45	0.08	226	1.46	169.7
3	45	0.11	291	1.23	181.2
4	75	0.05	208	1.46	175.3
5	75	0.08	240	1.24	186.2
6	75	0.11	281	1.16	195.2
7	130	0.05	162	1.31	187.5
8	130	0.08	216	1.28	198.6
9	130	0.11	268	1.32	206.0
10	190	0.05	164	1.22	197.6
11	190	0.08	213	1.40	205.3
12	190	0.11	260	1.14	215.6

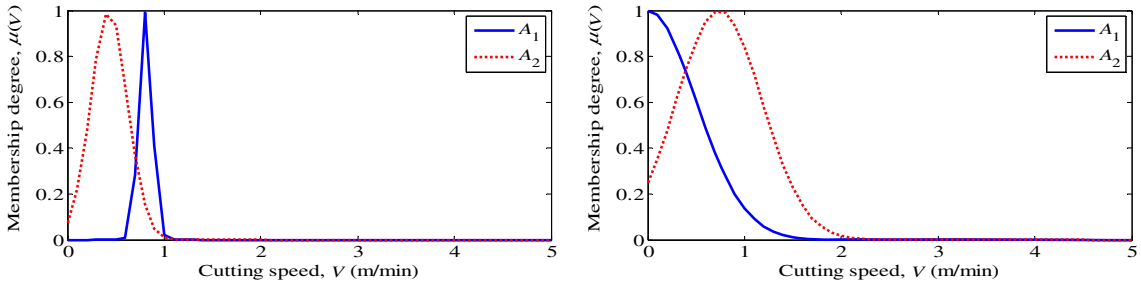

Fig. 5 Initial (*left*) and final (*right*) Gaussian MFs of input V

where α_1, α_2, α_3 are called learning constants; r_1 and r_2 are uniformly distributed random numbers in the range of [0–1]; ξ is a constriction factor; λ is a normally distributed random number vector. The last term in Eq. (7) reduces the possibility of stucking in a local minimum and it permits a more detailed search of the space. After the determination of particle velocity, the new position of the particle is updated using Eq. (8).

$$p_i(n+1) = p_i(n) + v_i(n+1) \tag{8}$$

The particle structure used in this study is represented by Eq. (9);

$$\vec{p}_i = [c_{1,1}\ \sigma_{1,1}\ c_{1,2}\ \sigma_{1,2}\ \ldots\ldots\ldots p_1\ q_1\ r_1\ t_1 \ldots\ldots\ldots p_{12}\ q_{12}\ r_{12}\ t_{12}] \tag{9}$$

where $c_{z,i}$ is the center of the ith MF for the zth input and $\sigma_{z,i}$ is the SD of the ith MF for the zth input. p_n, q_n, r_n, and t_n are rule parameters of the nth rule, respectively.

6 Modeling of surface roughness and cutting zone temperature based on ANFIS with PSO learning

In order to help the process planner in the selection of machining parameters, there is a need to find a technique that could able to predict the surface roughness and the cutting temperature. In this research, surface roughness and cutting zone temperature are predicted with the ANFIS as shown Fig. 3. For training the ANFIS, PSO learning algorithm is used to obtain a good predicting ability and its accuracy. The data set listed in Table 2 has been used to train ANFIS model using PSO algorithm.

The proposed ANFIS architecture has three inputs and two outputs. It consists of 12 fuzzy rules. Thus, the total number of premise (MF) and consequent (rule) parameters to be found is 60. After the training, the other set shown in Table 3 are used to verify the accuracy of the prediction model of surface roughness and cutting zone temperature.

The PSO-based ANFIS approach is implemented using a program. This program carries out modeling of surface roughness and cutting zone temperature based on cutting parameters including cutting speed and feedrate, and cutting force data obtained from experiments. At the beginning, experimental data are normalized into the range of [0 5]. Then, the procedure of PSO explained in previous section is operated to find optimal parameters of ANFIS prediction model. One thousand generations with a population size of 50 are used to run the algorithm. PSO swarm, a population of particles, is initialized randomly at the beginning of the learning phase. Establishing the ANFIS from the related particle, PSO is operated for the all training data, and pbest and gbest particle are found. By using them, present particles' velocities and positions are updated for the next generation. At the end of final generation, the optimal parameter values of ANFIS to predict surface roughness and cutting zone temperature are obtained. The PSO algorithm in the proposed model is run with a constriction factor of ξ= 0.76 and learning factors α_1=2.1, α_2=2.1 and α_3=10^{-3}.

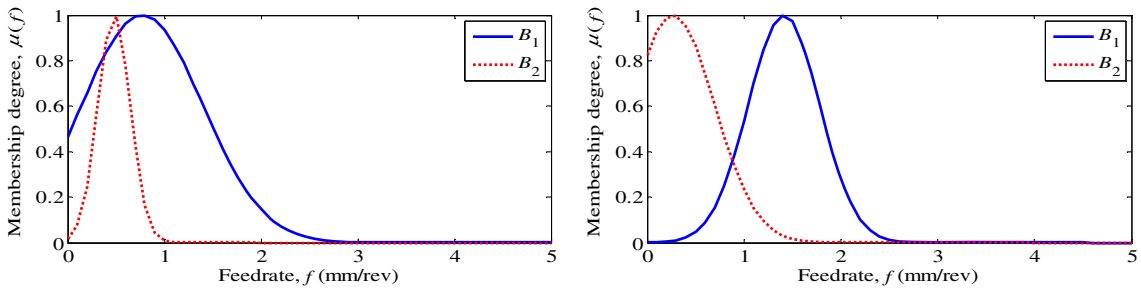

Fig. 6 Initial (*left*) and final (*right*) Gaussian MFs of input f

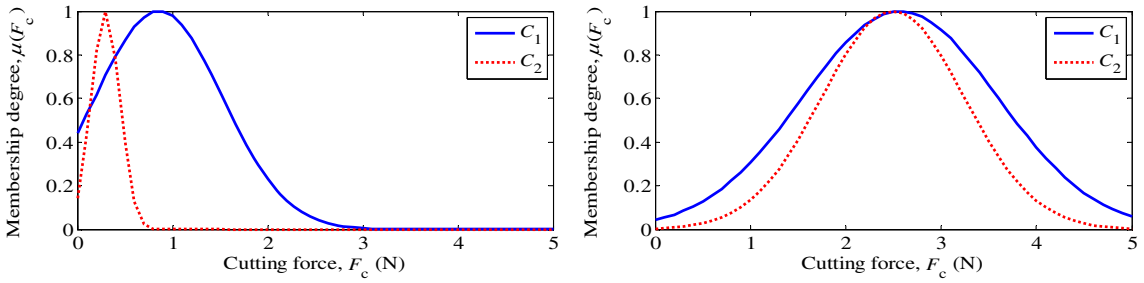

Fig. 7 Initial (*left*) and final (*right*) Gaussian MFs of input F_c

Table 4 Measured and predicted values of R_a and T_z for training data set

Experiment no.	V, (m/min)	f, (mm/rev)	F_c, (N)	R_a (μm)			T_z (°C)		
				Measured ($y_{i,e}$)	Predicted ($y_{i,p}$)	Error, ε (%)	Measured ($y_{i,e}$)	Predicted ($y_{i,p}$)	Error, ε (%)
1	30	0.05	174	1.60	1.59	0.63	135.9	144.4	6.25
2	30	0.08	232	1.48	1.48	0	150.5	154.3	2.52
3	30	0.11	258	1.39	1.39	0	161.3	160.8	0.31
4	55	0.05	177	1.51	1.49	1.32	161.8	150.8	6.80
5	55	0.08	236	1.32	1.32	0	180.4	169.2	6.21
6	55	0.11	292	1.18	1.17	0.85	190.8	196.3	2.88
7	110	0.05	159	1.37	1.36	0.73	181.7	179.9	0.99
8	110	0.08	222	1.32	1.32	0	192.7	195.2	1.30
9	110	0.11	272	1.21	1.18	2.48	201.3	200.3	0.50
10	220	0.05	162	1.14	1.13	0.88	204.9	205.6	0.34
11	220	0.08	216	1.37	1.37	0	210.6	212	0.66
12	220	0.11	251	1.24	1.25	0.81	229.7	228	0.74

Table 5 Measured and predicted values of R_a and T_z for testing data set

Experiment no.	V, (m/min)	f, (mm/rev)	F_c, (N)	R_a (μm)			T_z (°C)		
				Measured ($y_{i,e}$)	Predicted ($y_{i,p}$)	Error, ε (%)	Measured ($y_{i,e}$)	Predicted ($y_{i,p}$)	Error, ε (%)
1	45	0.05	168	1.53	1.49	2.61	148.6	142.7	3.97
2	45	0.08	226	1.46	1.38	5.48	169.7	160	5.72
3	45	0.11	291	1.23	1.19	3.25	181.2	188.3	3.92
4	75	0.05	208	1.46	1.39	4.79	175.3	180.4	2.91
5	75	0.08	240	1.24	1.24	0	186.2	181.4	2.58
6	75	0.11	281	1.16	1.18	1.72	195.2	195.8	0.31
7	130	0.05	162	1.31	1.26	3.82	187.5	192.6	2.72
8	130	0.08	216	1.28	1.36	6.25	198.6	204.5	2.97
9	130	0.11	268	1.32	1.19	9.85	206.0	203.3	1.31
10	190	0.05	164	1.22	1.18	3.28	197.6	202.2	2.33
11	190	0.08	213	1.40	1.34	4.29	205.3	208.9	1.75
12	190	0.11	260	1.14	1.19	4.39	215.6	215.5	0.05
Mean absolute error						4.14			2.55

7 Results and discussion

The established PSO-based ANFIS has been trained with the training data set. The Gaussian MF function is used to calculate membership degree for an input. The membership functions of each input of ANFIS are labeled as A_1, A_2, …, C_1, C_2 regions. Figures 5, 6, and 7 show the initial and final membership functions of the three input variables (V, f, and F_c) tuned by PSO learning stage. As seen in Fig. 5, the final membership function of V (cutting speed) has been exhibited a very limited variation in the related course at the end of training. It can be seen from Figs. 6 and 7 that, for the f (feedrate) and F_c (cutting force), the final membership functions after training obviously exhibit significant variations in the courses.

Table 4 shows comparison of measured and predicted values of surface roughness (R_a) and cutting zone temperature (T_z) for training data. It can be clearly seen from Table 4 that there is a quite high accuracy between the measured and predicted R_a and T_z values for training data set. After the training, testing data set is applied to the ANFIS system optimized by PSO. Outputs of ANFIS, the predicted values of R_a and T_z, are obtained. The values of surface roughness (R_a) and cutting zone temperature (T_z) predicted by the developed PSO-based ANFIS are given in Table 5 for comparison with the experimental testing data. As shown in Tables 4 and 5, the absolute percentage error (ε) is also computed for the predicted values of R_a and T_z according to Eq. (10), where $y_{i,e}$ and $y_{i,p}$ are the values of ith measured (experimental) and predicted (model) outputs, respectively.

$$\%\ \text{Absolute error}\ (\varepsilon) = \left|\frac{y_{i,e} - y_{i,p}}{y_{i,e}}\right| \times 100 \qquad (10)$$

Table 5 shows the performance of the predictions obtained from the proposed PSO-based ANFIS model. It can be seen that the mean absolute error of the predicted surface roughness is 4.14 %. That is, the prediction accuracy is as high as 95.86 %.

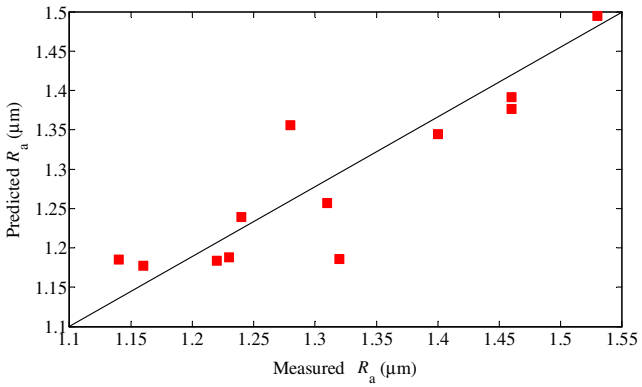

Fig. 8 Scatter diagram of measured R_a and predicted R_a for the testing data set

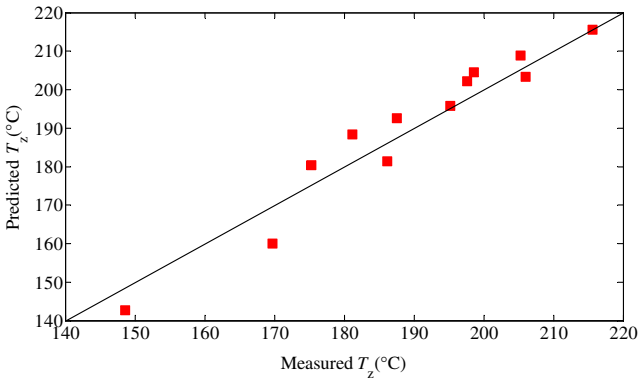

Fig. 9 Scatter diagram of measured T_z and predicted T_z for the testing data set

The mean absolute error and accuracy rate of the predicted cutting zone temperature is found as 2.55 and 97.45 % respectively. These results indicate that the training of ANFIS with PSO learning algorithm provides a higher accuracy rate for the prediction of surface roughness and cutting zone temperature.

The difference between the proposed model and the experimental results may be essentially attributed to high strength, high work hardening, high ductility, and poor thermal conductivity properties of austenitic stainless steels, characterized by high work hardening rate, high toughness, and low thermal conductivity. In addition, vibration and spindle run-out possibly affect the accuracy of predicted surface roughness. Furthermore, the chips bonded to the cutting tool during cutting have a considerable influence on the prediction of cutting zone temperature.

Figures 8 and 9 show the scatter diagrams of the predicted values and measured values of surface roughness and cutting zone temperature for testing data. Figure 8 shows that the predicted values of surface roughness are distributed around the line. Furthermore, the predicted values of surface roughness are not far from the experimental values. In Fig. 9, the cutting temperature distribution is less scattered than distribution of Fig. 8.

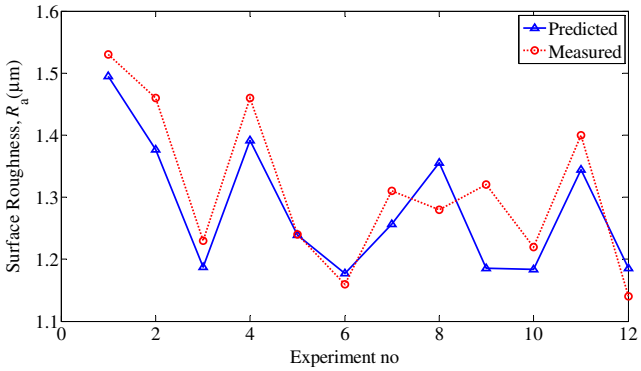

Fig. 10 The diagram of measured R_a and predicted R_a for the testing data set

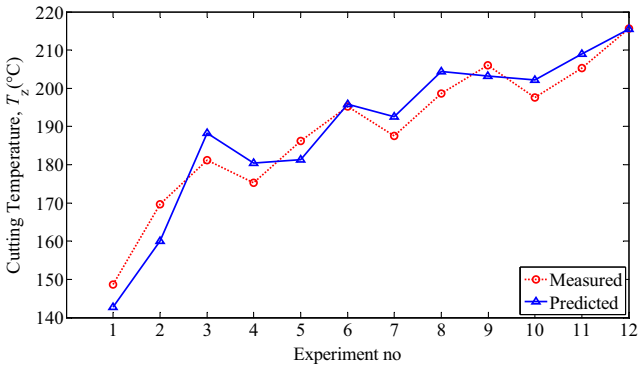

Fig. 11 The diagram of measured T_z and predicted T_z for the testing data set

Figures 10 and 11 compare the predicted values and measured values of surface roughness and cutting zone temperature for testing data. In Fig. 10, the predicted and measured surface roughness values are close to each other. But there is a slight error between the predicted values and measured values for the few testing data. Figure 11 shows that the predicted values are in good agreement with the experimental measured values for the cutting zone temperature, i.e., the error is very small.

From the analysis of Figures 8, 9, 10, and 11, the findings indicate that even though there is slight error between the predicted values and the measured values, PSO-based ANFIS provides an adequately accuracy considering properties of the machined material, as shown in Table 5.

8 Conclusions

This paper presents a PSO-based ANFIS system to accurately predict surface roughness and cutting zone temperature in dry turning of AISI 304 steel. PSO is run to determine the most suitable premise and consequent parameters of ANFIS. Cutting speed, feedrate, and measured cutting force data are used as model variables for training of PSO-based ANFIS. After the training stage, other data set, which is not used in the training data set, is used as testing data in order to validate the performance of ANFIS learned by PSO. Then, the surface roughness and the cutting temperature values predicted by PSO-based ANFIS are compared with the measured values in order to assess prediction ability of the PSO-based ANFIS. The following points can be drawn as conclusions from the above analysis:

- The predicting ability of the proposed approach is found to be 95.86 % for surface roughness and 97.45 % for cutting zone temperature. Consequently, the PSO-based ANFIS method effectively establishes the relationship between the inputs and the outputs. Once the cutting speed (V), the feedrate (f), and the cutting force (F_c) are given, surface roughness (R_a) and cutting zone temperature (T_z) can be easily predicted.
- From the results shown in Table 5, which reflects the system's prediction ability, the proposed approach is found to be satisfactory to predict surface roughness and cutting zone temperature for turning operations.
- The prediction ability and its accuracy make PSO-based ANFIS a powerful tool for industrial applications, and thus the performance characteristics can be successfully estimated through the proposed approach.
- PSO learning algorithm, considerably reducing computational time and manufacturing cost for turning, can be substitute for selecting of cutting parameters by trial and error. Thus, it can be obtained better product quality and high productivity with low cost.

References

1. Fernández-Abia AI, Barreiro J, López de Lacalle LN, Martínez S (2011) Effect of very high cutting speeds on shearing, cutting forces and roughness in dry turning of austenitic stainless steels. Int J Adv Manuf Technol 57:61–71
2. Fernández-Abia AI, Barreiro J, López de Lacalle LN, Martínez-Pellitero S (2012) Behavior of austenitic stainless steels at high speed turning using specific force coefficients. Int J Adv Manuf Technol. doi:10.1007/s00170-011-3846-9
3. Dolinšek S (2003) Work-hardening in the drilling of austenitic stainless steels. J Mater Process Technol 133:63–70
4. Korkut I, Kasap M, Ciftci I, Seker U (2004) Determination of optimum cutting parameters during machining of AISI304 austenitic stainless steel. Mater Des 25:303–305
5. Ciftci I (2006) Machining of austenitic stainless steels using CVD multi-layer coated cemented carbide tools. Tribol Int 39:565–569
6. Hashmi K, Graham ID, Mills B, Hashmi MSJ (2003) Adjustment approach for fuzzy logic model based selection of non-overlapping machining data in the turning operation. J Mater Process Technol 142:152–162
7. Nandi AK (2006) TSK-type FLC using a combined LR and GA: surface roughness prediction in ultra precision turning. J Mater Process Technol 178:200–210
8. Kirby ED, Chen JC, Zhang JZ (2006) Development of a fuzzy-nets-based in-process surface roughness adaptive control system in turning operations. Exp Syst Appl 30:592–604
9. Jiao Y, Lei S, Pei ZJ, Lee ES (2004) Fuzzy adaptive networks in machining process modeling: surface roughness prediction for turning operations. Int J Mach Tools Manuf 44:1643–1651
10. Ho SY, Lee KC, Chen SS, Ho SJ (2002) Accurate modeling and prediction of surface roughness by computer vision in turning operations using an adaptive neuro-fuzzy inference system. Int J Mach Tools Manuf 42:1441–1446
11. Abburi NR, Dixit US (2006) A knowledge-based system for the prediction of surface roughness in turning process. Rob Comput Integr Manuf 22:363–372
12. Kumar S, Kumar S, Prakash SR, Tiwari MK, Kumar SB (2007) Prediction of flow stress for carbon steels using recurrent self-organizing neuro fuzzy networks. Exp Syst Appl 32:777–788

13. Anand RB, Tiwari MK, Shankar R (2006) A self-organized neural network metamodelling and clonal selection optimization-based approach for the design of a manufacturing system. Int J Prod Res 44:1147–1170
14. Rai R, Kameshwaran S, Tiwari MK (2002) Machine-tool selection and operation allocation in FMS: solving a fuzzy goal-programming model using a genetic algorithm. Int J Prod Res 40:641–665
15. Tandon V, El-Mounayri H, Kishawy H (2002) NC end milling optimization using evolutionary computation. Int J Mach Tools Manuf 42:595–605
16. Lee TS, Ting TO, Lin YJ, Htay T (2007) A particle swarm approach for grinding process optimization analysis. Int J Adv Manuf Technol 33:1128–1135
17. Srinivas J, Giri R, Yang SH (2009) Optimization of multi-pass turning using particle swarm intelligence. Int J Adv Manuf Technol 40:56–66
18. Yıldız AR (2009) A novel particle swarm optimization approach for product design and manufacturing. Int J Adv Manuf Technol 40:617–628
19. Raja SB, Baskar N (2012) Application of particle swarm optimization technique for achieving desired milled surface roughness in minimum machining time. Exp Syst Appl 39:5982–5989
20. Jang JSR (1993) ANFIS: adaptive-network-based fuzzy inference system. IEEE Trans Syst Man Cybernet 23:665–685
21. Eberhart RC, Kennedy J (1995) A new optimizer using particle swarm theory. In Proceedings of the Sixth International Symposium on Micro Machine Human Science, Nagoya, Japan, pp 39–43
22. Çavuşlu MA, Karakuzu C, Karakaya F (2012) Neural identification of dynamic systems on FPGA with PSO learning. Appl Soft Comput 12:2707–2718